Entanglement Entropy Scaling Transition under Competing Monitoring Protocols

Mathias Van Regemortel, Ze-Pei Cian, Alireza Seif, Hossein Dehghani, and Mohammad Hafezi

Entanglement entropy scaling transition under competing monitoring protocols

Mathias Van Regemortel,[1, 2, *] Ze-Pei Cian,[1, 2] Alireza Seif,[1, 2] Hossein Dehghani,[1, 2] and Mohammad Hafezi[1, 2]

[1] *Joint Quantum Institute, College Park, 20742 MD, USA*
[2] *The Institute for Research in Electronics and Applied Physics,
University of Maryland, College Park, 20742 MD, USA*
(Dated: February 25, 2021)

Dissipation generally leads to the decoherence of a quantum state. In contrast, numerous recent proposals have illustrated that dissipation can also be tailored to stabilize many-body entangled quantum states. While the focus of these works has been primarily on engineering the non-equilibrium steady state, we investigate the build-up of entanglement in the quantum trajectories. Specifically, we analyze the competition between two different dissipation channels arising from two incompatible continuous monitoring protocols. The first protocol locks the phase of neighboring sites upon registering a quantum jump, thereby generating a long-range entanglement through the system, while the second destroys the coherence via a dephasing mechanism. By studying the unraveling of stochastic quantum trajectories associated with the continuous monitoring protocols, we present a transition for the scaling of the averaged trajectory entanglement entropies, from critical scaling to area-law behavior. Our work provides an alternative perspective on the measurement-induced phase transition: the measurement can be viewed as monitoring and registering quantum jumps, offering an intriguing extension of these phase transitions through the long-established realm of quantum optics.

While coupling a quantum system with the environment is often detrimental for preserving entanglement, dissipation can also be engineered and utilized to stabilize exotic and highly entangled many-body states [1–3]. With the development of recent experimental platform, such as circuit quantum electrodynamics (QED) [4–7] and Rydberg polaritons [8], strongly entangled photonic states can be engineered with reservoir engineering [9] and tailoring dissipation schemes [10–15].

Quantum phase transitions [16] typically come with different phases for entanglement entropy, as shown for the exemplary Bose-Hubbard model [17], where numerous works investigated the scaling of correlations with the system size [18–20]. Also local projective measurements of a quantum state destroy the entanglement generated by unitary evolution, which may lead to a phase transition of entanglement entropy across the system. A number of recent works have explored quantum circuits of random unitaries alternated with local measurements, and a phase transition was seen for the scaling of entanglement entropy [21–31]. Later a similar transition was reported for the stochastic trajectories from quantum systems under a local continuous-monitoring protocol, which induces an interplay with the entanglement from the unitary dynamics of the Hamiltonian [32–34]. More generally, it is worth investigating whether stochastic quantum trajectories, a well-established quantum optics formalism [35, 36], can provide more insight into measurement-induced phase transitions, by employing the possibility of registering the quantum jumps.

Here we present a scaling transition of entanglement entropy in a quantum system, governed entirely by dissipative dynamics – coming from the interplay of two continuous monitoring protocols – in the *absence* of unitary dynamics. In Fig. 1(a), we illustrate the model; a chain of bosonic modes, of length L and with open boundaries, is first monitored with a protocol that locks the phase of two adjacent sites with jump operators

$$d_j \equiv \left(a_j^\dagger + a_{j+1}^\dagger\right)\left(a_j - a_{j+1}\right), \tag{1}$$

where a_j $(a_j^\dagger)$ is the annihilation (creation) operator for the bosonic mode on site j [1]. The second monitoring protocol is dephasing, with jump operators

$$c_j \equiv a_j^\dagger a_j. \tag{2}$$

The rates of the monitoring for phase-locking d_j and dephasing c_j are given by Λ and Γ, respectively. We investigate the competition between the two monitoring schemes in terms of the *reduced* dephasing rate

$$\gamma \equiv \frac{\Gamma}{\Lambda}. \tag{3}$$

The continuous monitoring and the recording of the jumps is a crucial element of this work. While dissipation is often introduced to account for the decoherence of a quantum state, we elaborate specific implementation schemes that allow for the continuous tracking of the system in a circuit QED setup [37]. The random occurrence and detection of the quantum jumps (1) and (2) implies that the dynamics of a quantum state $|\psi(t)\rangle$ is inherently stochastic, as depicted in Fig. 1(b). To characterize the state of the system $|\psi(t)\rangle$, we use the entanglement entropy of a subsystem $\mathcal{A}$, a *state-dependent* quantity, which is evaluated as $S_\mathcal{A}[|\psi(t)\rangle] = -\text{Tr}\rho_\mathcal{A} \log \rho_\mathcal{A}$ with $\rho_\mathcal{A}$ the reduced density matrix of the state $|\psi(t)\rangle$ on $\mathcal{A}$. It is crucial that $S_\mathcal{A}$ is a strongly *nonlinear* function of the stochastic states $|\psi(t)\rangle$. As an immediate consequence, statistical averages of $S_\mathcal{A}[|\psi(t)\rangle]$ over the states can *not*
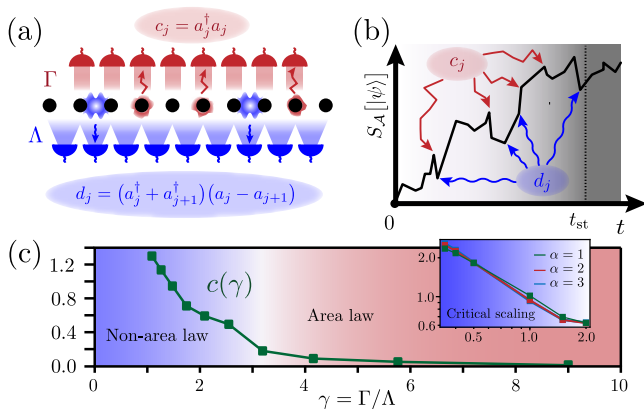
Figure 1. A schematic illustration of our setup and the scaling of trajectory entanglement entropy. (a) We analyze the stochastic evolution of the system under continuous monitoring with two competing monitoring protocols, characterized by the registering of jump operators d_j and c_j with rates Λ and Γ, respectively. (b) The quantum state $|\psi(t)\rangle$, starting from zero entropy, follows a stochastic trajectory under the continuous monitoring with d_j and c_j, which can be seen as random fluctuations of entanglement entropy of a subsystem. Over long enough times $t_{\rm st}$, the system is expected to converge to a steady state. (c) The fitting parameter from Eq. (6) $c(\gamma)$, with $\gamma \equiv \Gamma/\Lambda$, obtained from fitting to a system with $L = 32$, showing a transition from area law (high γ) to non-area law (low γ). The inset shows $c(\gamma)$, derived from $c_\alpha(\gamma)$ from the Renyi entropy of order α for CFT's (4). The coincidence of the $c(\gamma)$ curves for different order α for small γ is suggestive for a phase of critical scaling, where the effective central charge shows the onset of a power-law divergence as function of γ.

be retrieved from a master-equation approach. This in stark contrast with linear quantities, such as operator expectation values $\langle O \rangle_t = \langle \psi(t) | O | \psi(t) \rangle$ [35, 38], which converge to the master equation and exhibit a notion of ergodicity [39] and thermalization [40, 41]. Importantly, there is a convergence time $t_{\rm st}$ for $S_{\mathcal{A}}$, after which the stochastic state $|\psi(t)\rangle$ is sampled from a steady-state distribution.

We present a scaling transition for the averaged entanglement entropy of stochastic states, after some evolution time, across a critical value of the reduced dephasing rate (3), as presented in Fig. 1(c). When phase-locking dominates, the state is superfluid and entanglement entropy has a strong dependence on subsystem size. We report the critical scaling, characterized by an effective central charge $c(\gamma)$ (green line). While an appropriate scaling analysis is difficult due to numerical constraints, our hypothesis is motivated by the results on the inset of Fig. 1c: the effective curvature c_α found for averaged higher-order Rényi entropies $S_\alpha = 1/(1-\alpha) \log \text{Tr}\rho^\alpha$ follows the universal scaling from conformal field theory (CFT)

[42, 43]

$$c_\alpha(\gamma) = \frac{c(\gamma)}{2}\left(1 + \frac{1}{\alpha}\right), \tag{4}$$

and the effective central charge $c(\gamma)$ shows the onset of a power-law divergence for $\gamma \to 0$. While the *full* master equation in this regime is expected to converge to a mixed steady state with a volume law, there is no *a priori* reason why *trajectory* entanglement entropy should follow the same scaling.

When dephasing becomes more important (higher γ), the scaling changes to an area law, marked by $c(\gamma) \approx 0$. Intuitively, the transition can be further understood from an order parameter in a simple Gutzwiller picture, elaborated in [37]. In circuit-models, two incompatible types of measurements *without* unitary entangling gates can also lead to a scaling transition for entanglement entropy [44, 45]. Our work aims to extend the recent understanding of a measurement-induced phase transition, as seen in discrete random circuits, to the stochastic trajectories of an unraveling associated with the continuous monitoring of a quantum system.

Stochastic trajectories.– The system dynamics is fully governed by the two competing monitoring protocols. A state $|\psi(t)\rangle$ then follows a stochastic trajectory, as was originally introduced in the seminal works [35, 38] as a way to sample the master equation of an open quantum system. Whereas the *unraveling* for sampling a master equation is not unique, here it relates unequivocally to the monitoring protocol presented in Fig. 1(a)-(b), thereby relying explicitly on the hypothesis of detector-dependent stochastic pure-state dynamics [36].

The sampling of quantum trajectories from the continuous monitoring goes as follows. At time t, we evaluate whether there is a jump in the differential time interval $[t, t + \Delta t]$ by evaluating the probability $\Delta p = \sum_{j=1}^{L-1} \Delta p_j^{(d)} + \sum_{j=1}^{L} \Delta p_j^{(c)}$, a summation over the probabilities $\Delta p_j^{(d)}$ and $\Delta p_j^{(c)}$ of the jumps d_j and c_j to occur, with $\Delta p^{(b)} = \gamma^{(b)} \langle \psi(t) | b^\dagger b | \psi(t) \rangle \Delta t$ and $\gamma^{(b)} = \{\Lambda, \Gamma\}$, accordingly.

If no jump is detected (probability $1 - \Delta p$) we evolve the state over Δt with the anti-Hermitian Hamiltonian $H_{\rm eff} = -\frac{i\Lambda}{2}\sum_{j=1}^{L-1} d_j^\dagger d_j - \frac{i\Gamma}{2}\sum_{j=1}^{L} c_j^\dagger c_j$. If a jump is recorded (probability Δp), we select one $b \in \{d_j, c_j\}$ with probabilities $\Delta p_j^{(d)}$ or $\Delta p_j^{(c)}$, respectively, to evaluate $|\psi(t + \Delta t)\rangle = b|\psi(t)\rangle$.

After each time step Δt, the state $|\psi(t)\rangle$ is normalized to simulate the stochastic evolution of $|\psi_i(t)\rangle$ in the monitoring scheme. Importantly, both detection (probability Δp) as well as *absence* of a jump (probability $1 - \Delta p$) in Δt yields information about the state of the system to an observer. This was illustrated in several recent experiments to monitor the stochastic evolution of a superconducting qubit [46–49] and how simultaneously monitoring dephasing and relaxation leads to an interplay [50].

The phase-locking (1) stabilizes a pure Bose-Einstein Condensate (BEC) dark state with long-range entanglement, where all L particles are injected in the zero-momentum mode; $|D\rangle = (a_{k=0}^\dagger)^L|0\rangle$, with $a_k^\dagger$ the creation operator of a photon with momentum k [1, 2], while dephasing (2) directs the system to a product of local Fock states with zero entanglement.

While the local $U(1)$ symmetry is broken by the phase locking (1), a global $U(1)$ symmetry is present in our system; both jumps d_j (1) and c_j (2) conserve the total particle number. For the upcoming analysis we fix the filling factor $n = 1$ and the evolution starts from the Fock state $|\psi(t=0)\rangle = |...1111...\rangle$.

Gutzwiller approach.– Given a stochastic trajectory state $|\psi(t)\rangle$, upon taking the thermodynamic limit $L \to \infty$, we can study the dynamics of on-site observables in the Gutzwiller approximation by considering a mean-field coupling to neighboring sites for the single-site reduced density matrix [51, 52]. An effective single-site Liouvillian can be constructed for the Gutzwiller master equation of the reduced density matrix after averaging over trajectories. A full numerical analysis of the mean-field *order parameter* $\alpha \equiv \langle a \rangle$ shows that it vanishes across a critical value $\gamma_c^{(\mathrm{GW})} \approx 3$, as such providing a suggestive sign for a trajectory transition, see [37].

Trajectory entanglement entropy.– We focus on evaluating the Von Neumann entanglement entropy of the trajectory states from a system of size L, $|\psi_L\rangle$, in a subsystem $\mathcal{A}$ containing l sites from the left: $S(l)[|\psi_L\rangle] = -\mathrm{Tr}[\rho_\mathcal{A} \log \rho_\mathcal{A}]$, with $\rho_\mathcal{A} = \mathrm{Tr}_\mathcal{B}|\psi_L\rangle\langle\psi_L|$ the reduced density matrix of $\mathcal{A}$ and $\mathcal{B}$ containing the remaining $L - l$ sites. We evaluate the averaged entanglement entropy of a set of M stochastic trajectory states $|\psi_L^{(\gamma)}(t)\rangle_i$, $i \in [1, M]$, at time t in a system with reduced dephasing rate γ (3),

$$\overline{S}_L^{(\gamma)}(l, t) = \frac{1}{M} \sum_{i=1}^M S(l)[|\psi_L^{(\gamma)}(t)\rangle_i]. \qquad (5)$$

Numerical results.– We use Matrix Product States (MPS) [53] to sample the stochastic quantum states [54] with the C++ package *ITensor* [55].

In Fig. 2, the scaling of the averaged entanglement entropy $\bar{S}_L^{(\gamma)}(l)$ for trajectories sampled from the steady state is illustrated for three parameters l (a), L (b) and γ (c). In Fig. 2(a) we see that the curves $\bar{S}_L^{(\gamma)}(l)$ show a transition from a strong concave behavior as function of l when phase-locking dominates (black, blue and orange line) to a regime with an area-law behavior (green and red line). After numerical analysis, we identify the scaling of the curves in the phase-locking regime as logarithmic, reminiscent of the scaling of entanglement entropy for ground states of critical Hamiltonians with open boundary conditions [17], given by a result from CFT [42],

$$\bar{S}_L^{(\gamma)}(l) = \frac{c(\gamma)}{6} \log\left[\frac{2L}{\pi} \sin\left(\frac{\pi l}{L}\right)\right] + s_0(\gamma). \qquad (6)$$
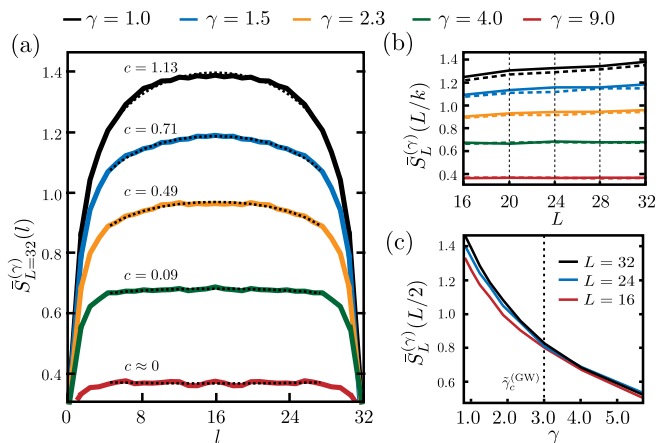

Figure 2. Different scalings of $\bar{S}_L^{(\gamma)}(l)$ from averaging over 10000 steady-state trajectory states. (a) The scaling of $\bar{S}_{L=32}^{(\gamma)}(l)$ as function of l for different values of the reduced dephasing γ. A transition is seen from critical scaling (black, blue, orange lines) to an area law (green and red line), as obtained from the effective central charges $c(\gamma)$ found by fitting (dotted lines) the functional form (6) (b) The scaling of $\bar{S}_L^{(\gamma)}(L/2)$ (solid) and $\bar{S}_L^{(\gamma)}(L/4)$ (dashed) as function of L. (c) The dependence of $\bar{S}_L^{(\gamma)}(L/2)$ on γ for different system sizes L; we distinguish a critical point γ_c where the lines start to coincide, close to the Gutzwiller critical point $\gamma_c \approx 3$.

Here $c(\gamma)$ is the effective central charge and $s_0(\gamma)$ the residual entropy.

A fitting procedure (dotted lines) with the functional form (6) gives the parameters $c(\gamma)$ (indicated above the curve) and $s_0(\gamma)$, in close agreement with the numerical results (solid lines). In Fig. 1(c) we summarize our key result: the fitted central charge shows a transition from a nonzero value to zero upon increasing the effective dephasing rate γ. Consequently, we report a transition from critical scaling of entanglement (6) to an area law, characterized by $c(\gamma) = 0$, which has a plateau value $s_0(\gamma)$ for the bulk entanglement entropy. In the limit $\gamma \to \infty$ no entanglement can build up and $\bar{S}_L^{(\gamma)}(l) \to 0$, so that also $s_0(\gamma) \to 0$.

In the inset of 1(c), we analyze the critical behavior more closely by investigating Rényi entropies of order α, which satisfy the universal relation for CFT (4) [42, 43]. The central charge $c(\gamma)$ is shown, as obtained from $c_\alpha(\gamma)$ of the Rényi entropy S_α, averaged over steady-state trajectories, analogous to (5). We conclude that the central charges $c(\gamma)$ coincide within numerical precision, as such retrieving the universality relation from CFT and confirming the reported critical scaling. Moreover, as we let $\gamma \to 0$, the central charge $c_1(\gamma)$ appears to show a power-law divergence, as was also seen for free fermion trajectories with dephasing [34].

The exact critical γ_c for the scaling transition is difficult to extract from our numerical data. We are computationally limited (mainly the finite bond dimension and

local Fock-space truncation of the MPS) to sampling system sizes of $L \lesssim 32$ with $\gamma \gtrsim 0.35$, making a finite-size scaling analysis difficult. We also leave it as an open question whether the power-law scaling for $c(\gamma)$ persists or stabilizes to a finite value at $\gamma > 0$.

Alternatively, the scaling of entanglement entropy with system size L can be studied, as shown in Fig. 2(b) for the averaged half-chain entanglement entropy $\bar{S}_L^{(\gamma)}(L/2)$ (solid lines) and quarter-chain entanglement entropy $\bar{S}_L^{(\gamma)}(L/4)$ (dashed lines). When γ is below the critical point (black, blue and orange line), a monotonous growth of entanglement entropy is observed when L is increased and a significant difference can be distinguished between the curves of half-chain and quarter-chain entanglement entropy, relating back to the critical scaling of the lines seen in Fig. 2(a). For larger γ, when dephasing dominates (green and red lines), both half-chain and quarter-chain entropy coincide and remain constant as a function of system size, thus reflecting the area law with a plateau of the residual entropy $s_0(\gamma)$ when $c(\gamma) \approx 0$ in (6), shown in Fig. 2(a).

To study the behavior across the transition, we show in Fig. 2(c) the steady-state scaling of half-chain entropy $\bar{S}_L^{(\gamma)}(L/2)$ as function of γ for different system sizes L. When γ is below γ_c, the critical point we find in the Gutzwiller approach [37], the curves for different L fall apart. Upon increasing γ, $\bar{S}_L^{(\gamma)}(L/2)$ decreases for all L and when a critical point is reached, close to $\gamma_c^{(\mathrm{GW})} = 3$ from the Gutzwiller analysis [37], the curves for different L converge. For higher γ the curves coincide, which confirms that $\bar{S}_L^{(\gamma)}(L/2)$ is uniform for different system sizes L in the dephasing regime, shown in Fig. 2(b).

We believe that we have strong indications for critical scaling, in particular by satisfying (4). However, to unambiguously exclude the possibility of a volume law over critical scaling for $\gamma \to 0$, a thorough analysis of larger system sizes L is required. Also topological entanglement entropy [29] could be a promising route. However, this quantity is prohibitively difficult to obtain with MPS simulations.

Finally, Fig. 3 shows the evolution of half-chain entanglement entropy $\bar{S}_L^{(\gamma)}(L/2, t)$ over time for $L = 32$ (solid lines) and $L = 16$ (dashed lines) for different values of γ. Starting from a zero entropy state, we let the system evolve and sample trajectories to see the rise in entanglement entropy. A saturation time t_{st} is found where $\bar{S}_L^{(\gamma)}(L/2, t)$ converges to a steady-state value, schematically depicted in Fig. 1(b), which depends on both the system size L and reduced dephasing rate γ. When dephasing is dominant (red lines), $\bar{S}_L^{(\gamma)}(L/2, t)$ rapidly stabilizes and the curves for different L are indistinguishable from each other, as expected for the area law. In the regime where phase-locking dominates (blue and black lines) the convergence is much slower, since entanglement
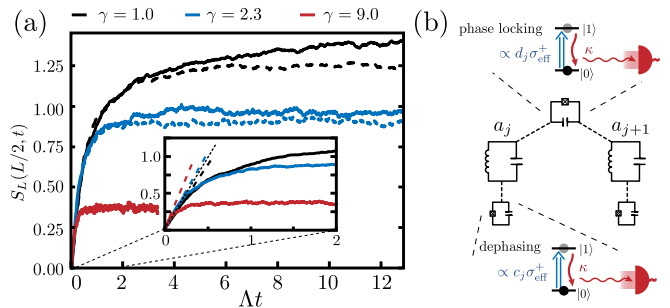

Figure 3. The time evolution of $\bar{S}_L^{(\gamma)}\left(\frac{L}{2}, t\right)$ in time for $L = 32$ (solid) and $L = 16$ (dashed) obtained from averaging over 500 trajectories. Below the critical point (black and blue lines) entanglement entropy for different L converges to different values, while above (red lines) it converges to the same steady value. In the inset we show the short-time behavior and see that the initial growth is linear (dashed lines), with a rate close to $\frac{\Lambda}{2}$ (dotted line). (b) A schematic of the setup proposed for the experimental implementation. The cavities are coupled 2-by-2 to disspative ancilla spins for the phase locking jumps and each cavity is coupled to another ancilla for the dephasing. Registering spontaneous spin decays in the ancillae allows for the registering of cavity jumps.

spreads between distant sites. Different system sizes L (solid vs. dotted lines) now converge to different steady-state values, reflecting the critical scaling of $\bar{S}_L^{(\gamma)}(l)$ (6), previously shown more accurately in Fig. 2(b).

The initial growth, shown in the inset of Fig. 3, is close to linear (dashed lines), i.e. $\bar{S}_L^{(\gamma)}(L/2, t) = \kappa t$, with $\kappa \approx \frac{\Lambda}{2}$ (dotted line). The growth of trajectory entanglement entropy is thus reminiscent of the entanglement growth after a quench, where also an initial linear behavior is seen which saturates to a steady value. [56]

Circuit QED implementation.– Although originally presented in a cold-atom context [1], phase-locking (1) can also be engineered in circuit QED [57]. We propose the realization of a coupling between two adjacent cavities and an ancilla qubit $H_{\mathrm{eff}} \approx g_{\mathrm{eff}} d_j \sigma_j^x$, with $\sigma^x = \sigma^+ + \sigma^-$. If the qubit is very lossy, registering a spontaneous qubit decay corresponds to detecting a phase-locking jump. In [37] we elaborate a scheme to engineer H_{eff} by coupling the cavities 2-by-2 to a driven ancilla with an anharmonic level structure, such as a fluxonium qubit [58].

While dephasing noise (2) is ubiquitous in quantum systems [40, 59–62], it is generally not possible to monitor the environment that induces the noise. In our approach, however, we keep track of individual trajectories, an essential aspect, and we propose a scheme to engineer dephasing processes by coupling each cavity to another lossy ancilla with $\sim a_j^\dagger a_j \sigma_x$. Upon registering an ancilla emission jump, one can infer the occurrence of a dephasing jump c_j, see [37]. This is in contrast with [48], where a coupling $H \sim a^\dagger a \sigma_z$ was used to monitor the cavity

parity with qubit measurements to register photon decay. In our proposal, the ancilla serves both to engineer *and* to register the dephasing jump c_j.

In Fig. 3(b) we show a schematic of the proposal for the simultaneous realization of the two monitoring protocols by coupling two ancillae to each cavity, see [37].

Conclusions and outlook.– We have investigated the scaling transition for entanglement entropy averaged over trajectory states $\bar{S}^{(\gamma)}(l)$ from two competing monitoring protocols. We report a transition in the steady-state trajectory entanglement entropy from area law to critical scaling (6), where the central charge satisfies the relation for CFT's 4 for different Rényi entropies.

Investigating larger filling factor $n > 1$ would allow for the study of entanglement entropy in different $U(1)$ charge sectors [63, 64]. The unraveling of a master equation is not unique and, as such, entanglement depends on the monitoring [65]. It would be fascinating to investigate if a similar transition can be seen for different unravelings within the same master equation. Since trajectory entanglement entropy is a quantity that is challenging (if not impossible) to measure directly in experiment – it requires identical copies of the same stochastic state [66, 67] – investigating if there could be a local probe to witness the transition, like in circuit models [27], is an exciting question. Finally, it would be intriguing to see if quantum states can be stabilized with feedback from jumps in a continuous monitoring scheme [68].

———————

* mvanrege@umd.edu

[1] S. Diehl, A. Micheli, A. Kantian, B. Kraus, H. Büchler, and P. Zoller, Nature Physics **4**, 878 (2008).

[2] B. Kraus, H. P. Büchler, S. Diehl, A. Kantian, A. Micheli, and P. Zoller, Physical Review A **78**, 042307 (2008).

[3] F. Verstraete, M. M. Wolf, and J. I. Cirac, Nature physics **5**, 633 (2009).

[4] A. Blais, J. Gambetta, A. Wallraff, D. I. Schuster, S. M. Girvin, M. H. Devoret, and R. J. , Physical Review A **75**, 032329 (2007).

[5] R. Schoelkopf and S. Girvin, Nature **451**, 664 (2008).

[6] A. A. Houck, H. E. Türeci, and J. Koch, Nature Physics **8**, 292 (2012).

[7] M. Kounalakis, C. Dickel, A. Bruno, N. K. Langford, and G. A. Steele, npj Quantum Information **4**, 1 (2018).

[8] M. Saffman, T. G. Walker, and K. Mølmer, Reviews of modern physics **82**, 2313 (2010).

[9] J. Poyatos, J. I. Cirac, and P. Zoller, Physical review letters **77**, 4728 (1996).

[10] H. Weimer, M. Müller, I. Lesanovsky, P. Zoller, and H. P. Büchler, Nature Physics **6**, 382 (2010).

[11] M. J. Kastoryano, F. Reiter, and A. S. Sørensen, Physical review letters **106**, 090502 (2011).

[12] J. Cho, S. Bose, and M. Kim, Physical review letters **106**, 020504 (2011).

[13] J. T. Barreiro, M. Müller, P. Schindler, D. Nigg, T. Monz, M. Chwalla, M. Hennrich, C. F. Roos, P. Zoller, and R. Blatt, Nature **470**, 486 (2011).

[14] F. Reiter, L. Tornberg, G. Johansson, and A. S. Sørensen, Physical Review A **88**, 032317 (2013).

[15] Z.-P. Cian, G. Zhu, S.-K. Chu, A. Seif, W. DeGottardi, L. Jiang, and M. Hafezi, Physical review letters **123**, 063602 (2019).

[16] S. Sachdev, Handbook of Magnetism and Advanced Magnetic Materials (2007).

[17] A. M. Läuchli and C. Kollath, Journal of Statistical Mechanics: Theory and Experiment **2008**, P05018 (2008).

[18] M. P. Fisher, P. B. Weichman, G. Grinstein, and D. S. Fisher, Physical Review B **40**, 546 (1989).

[19] T. D. Kühner and H. Monien, Physical Review B **58**, R14741 (1998).

[20] S. Ejima, H. Fehske, and F. Gebhard, EPL (Europhysics Letters) **93**, 30002 (2011).

[21] A. Nahum, J. Ruhman, S. Vijay, and J. Haah, Physical Review X **7**, 031016 (2017).

[22] Y. Li, X. Chen, and M. P. Fisher, Physical Review B **98**, 205136 (2018).

[23] B. Skinner, J. Ruhman, and A. Nahum, Physical Review X **9**, 031009 (2019).

[24] A. Chan, R. M. Nandkishore, M. Pretko, and G. Smith, Physical Review B **99**, 224307 (2019).

[25] R. Vasseur, A. C. Potter, Y.-Z. You, and A. W. W. Ludwig, Phys. Rev. B **100**, 134203 (2019).

[26] S. Choi, Y. Bao, X.-L. Qi, and E. Altman, Physical Review Letters **125**, 030505 (2020).

[27] M. J. Gullans and D. A. Huse, Physical review letters **125**, 070606 (2020).

[28] C.-M. Jian, Y.-Z. You, R. Vasseur, and A. W. Ludwig, Physical Review B **101**, 104302 (2020).

[29] A. Zabalo, M. J. Gullans, J. H. Wilson, S. Gopalakrishnan, D. A. Huse, and J. Pixley, Physical Review B **101**, 060301 (2020).

[30] Y. Bao, S. Choi, and E. Altman, Physical Review B **101**, 104301 (2020).

[31] O. Shtanko, Y. A. Kharkov, L. P. García-Pintos, and A. V. Gorshkov, arXiv preprint arXiv:2004.06736 (2020).

[32] Y. Fuji and Y. Ashida, Phys. Rev. B **102**, 054302 (2020).

[33] X. Cao, A. Tilloy, and A. De Luca, SciPost Physics **7**, 024 (2019).

[34] O. Alberton, M. Buchhold, and S. Diehl, arXiv preprint arXiv:2005.09722 (2020).

[35] J. Dalibard, Y. Castin, and K. Mølmer, Physical review letters **68**, 580 (1992).

[36] H. M. Wiseman and J. M. Gambetta, Physical review letters **108**, 220402 (2012).

[37] see Supplemental Material.

[38] R. Dum, A. Parkins, P. Zoller, and C. Gardiner, Physical Review A **46**, 4382 (1992).

[39] B. Kuemmerer and H. Maassen, Journal of Physics A: Mathematical and General **37**, 11889 (2004).

[40] J. Schachenmayer, L. Pollet, M. Troyer, and A. J. Daley, Physical Review A **89**, 011601 (2014).

[41] Y. Ashida, K. Saito, and M. Ueda, Physical review letters **121**, 170402 (2018).

[42] P. Calabrese and J. Cardy, Journal of Statistical Mechanics: Theory and Experiment **2004**, P06002 (2004).

[43] M. Fagotti, P. Calabrese, and J. E. Moore, Physical Review B **83**, 045110 (2011).

[44] A. Lavasani, Y. Alavirad, and M. Barkeshli, arXiv preprint arXiv:2004.07243 (2020).

[45] M. Ippoliti, M. J. Gullans, S. Gopalakrishnan, D. A. Huse, and V. Khemani, arXiv preprint arXiv:2004.09560 (2020).

[46] K. Murch, S. Weber, C. Macklin, and I. Siddiqi, Nature **502**, 211 (2013).

[47] S. Weber, A. Chantasri, J. Dressel, A. N. Jordan, K. Murch, and I. Siddiqi, Nature **511**, 570 (2014).

[48] L. Sun, A. Petrenko, Z. Leghtas, B. Vlastakis, G. Kirchmair, K. Sliwa, A. Narla, M. Hatridge, S. Shankar, J. Blumoff, *et al.*, Nature **511**, 444 (2014).

[49] Z. K. Minev, S. O. Mundhada, S. Shankar, P. Reinhold, R. Gutiérrez-Jáuregui, R. J. , M. Mirrahimi, H. J. Carmichael, and M. H. Devoret, Nature **570**, 200 (2019).

[50] Q. Ficheux, S. Jezouin, Z. Leghtas, and B. Huard, Nature communications **9**, 1 (2018).

[51] J. Lebreuilly, C. Aron, and C. Mora, Physical review letters **122**, 120402 (2019).

[52] W. Casteels and M. Wouters, Physical Review A **95**, 043833 (2017).

[53] D. Perez-Garcia, F. Verstraete, M. Wolf, and J. Cirac, Quantum Information & Computation **7**, 401 (2007).

[54] A. J. Daley, Advances in Physics **63**, 77 (2014).

[55] ITensor Library (version 2.0.11) http://itensor.org.

[56] P. Calabrese and J. Cardy, Journal of Statistical Mechanics: Theory and Experiment **2005**, P04010 (2005).

[57] D. Marcos, A. Tomadin, S. Diehl, and P. Rabl, New Journal of Physics **14**, 055005 (2012).

[58] S. Girvin, M. Devoret, and R. Schoelkopf, Physica Scripta **2009**, 014012 (2009).

[59] M. Boissonneault, J. M. Gambetta, and A. Blais, Physical Review A **79**, 013819 (2009).

[60] A. Sears, A. Petrenko, G. Catelani, L. Sun, H. Paik, G. Kirchmair, L. Frunzio, L. Glazman, S. Girvin, and R. Schoelkopf, Physical Review B **86**, 180504 (2012).

[61] Y. Yanay and E. J. Mueller, Physical Review A **90**, 023611 (2014).

[62] J.-S. Bernier, R. Tan, C. Guo, C. Kollath, and D. Poletti, Phys. Rev. B **102**, 115156 (2020).

[63] M. Goldstein and E. Sela, Physical review letters **120**, 200602 (2018).

[64] S. Murciano, G. Di Giulio, and P. Calabrese, Journal of High Energy Physics **2020**, 1 (2020).

[65] H. Nha and H. Carmichael, Physical review letters **93**, 120408 (2004).

[66] A. Elben, B. Vermersch, C. F. Roos, and P. Zoller, Physical Review A **99**, 052323 (2019).

[67] H. Pichler, G. Zhu, A. Seif, P. Zoller, and M. Hafezi, Physical Review X **6**, 041033 (2016).

[68] H. M. Wiseman, Physical Review A **49**, 2133 (1994).

[69] J. Towns, T. Cockerill, M. Dahan, I. Foster, K. Gaither, A. Grimshaw, V. Hazlewood, S. Lathrop, D. Lifka, G. D. Peterson, R. Roskies, J. Scott, and N. Wilkins-Diehr, Computing in Science & Engineering **16**, 62 (2014).

[70] N. A. Nystrom, M. J. Levine, R. Z. Roskies, and J. R. Scott, in *Proceedings of the 2015 XSEDE Conference: Scientific Advancements Enabled by Enhanced Cyberinfrastructure*, XSEDE '15 (ACM, New York, NY, USA, 2015) pp. 30:1–30:8.